



On the extent of mantle hydration caused by plate bending



Jun Korenaga*

Department of Geology and Geophysics, Yale University, New Haven, CT 06520, USA

ARTICLE INFO

Article history:

Received 15 February 2016
 Received in revised form 15 September 2016
 Accepted 10 October 2016
 Available online 21 October 2016
 Editor: B. Buffett

Keywords:

global water cycle
 thermal cracking
 intermediate-depth earthquakes

ABSTRACT

When bent at subduction zones, oceanic plates are damaged by normal faulting, and this bending-related faulting is widely believed to cause deep mantle hydration, down to ~20–30 km deep. The buoyancy of water (or equivalently, confining pressure), however, makes it difficult to bring water down even if faulting is deep. Extension associated with plate bending generates negative dynamic pressure, but the magnitude of such dynamic pressure is shown to be insufficient to overcome confining pressure. Seismic velocity anomalies that have been used to infer the extent of mantle hydration are reviewed, and it is suggested that small crack-like porosities, which can be produced by thermal cracking and further enhanced by bending-related faulting, is sufficient to explain such velocity anomalies. The presence of such porosities, however, does not necessarily lead to the substantial hydration of oceanic plates because of confining pressure. Whereas the depth extent of bending-generated porosities is uncertain, the theory of thermal cracking can be used to place a lower bound on the amount of water contained in the slab mantle (0.03–0.07 wt% H₂O), and this lower bound is suggested to be more than sufficient to explain the lower-plane earthquakes of the double seismic zone by dehydration embrittlement.

© 2016 Elsevier B.V. All rights reserved.

1. Introduction

Oceanic plates are often thought to be deeply faulted when they are bent at subduction zones (Christensen and Ruff, 1988; Seno and Yamanaka, 1996; Ranero et al., 2003). The alteration of an oceanic plate by seawater takes place as soon as the plate forms at a mid-ocean ridge, but bending at a subduction zone could potentially hydrate the plate down to the depths of several tens of kilometers if faulting is correspondingly deep (Peacock, 2001). The extent of hydration in subducting plates is important for the deep water cycle (e.g., Rüpke et al., 2004), and quite a few observational and theoretical studies on this issue have been published in recent years (e.g., Grevemeyer et al., 2007; Faccenda et al., 2008, 2009; Van Avendonk et al., 2011; Garth and Rietbrock, 2014; Naif et al., 2015).

Water is, however, buoyant with respect to silicate rocks, and given the magnitude of confining pressure (i.e., the difference between lithostatic and hydrostatic pressures), which increases at the rate of ~23 MPa km⁻¹, it is not obvious how deeply water can infiltrate even when faulting is deep. Peacock (2001) suggested that downward water transport might be possible by seismic pumping (Sibson et al., 1975), which is based on the dilatancy-diffusion hypothesis for shallow earthquakes (Scholz et al., 1973). As the

validity of the dilatancy-diffusion hypothesis is questionable in a number of aspects (e.g., Main et al., 2012), it has become difficult to defend the original seismic pumping mechanism. Instead of dilatancy, tectonic deformation may be able to generate a sufficient hydraulic gradient to allow downward water transport (e.g., McCaig, 1988), and based on numerical modeling, Faccenda et al. (2009) suggested that plate bending could yield strongly negative ‘tectonic’ pressure that promotes deep mantle hydration. As shown in this paper, however, the generation of such negative pressure may be in direct conflict with the dynamics of brittle deformation.

Observational efforts to constrain the extent of hydration have been notable particularly in the field of active-source seismology (e.g., Ranero and Sallarès, 2004; Grevemeyer et al., 2007; Van Avendonk et al., 2011), with conclusions invariably in favor of the deep hydration of incoming plates. The interpretation of estimated seismic velocity structure in these studies, however, is not unique and seems to have overlooked an important complication caused by the topology of porosity (e.g., Korenaga et al., 2002). A 10% reduction in the *P*-wave velocity of mantle rocks, for example, can be caused by ~20% serpentinization (equivalent to ~2 wt% H₂O) or by ~0.1% of crack-like residual porosity (equivalent to ~0.03 wt% H₂O).

The purpose of this paper is three-fold: (1) derive a theoretical bound on dynamic pressure caused by brittle deformation, (2) examine the degree of nonuniqueness associated with the interpretation of crustal and mantle seismic velocities, and (3) estimate the likely extent of mantle hydration by assembling relevant geo-

* Fax: +1 203 432 3134.

E-mail address: jun.korenaga@yale.edu.

physical observations. In doing so, I will also discuss the potential role of thermal cracking (Korenaga, 2007b) in mantle hydration as well as the origin of intermediate-depth earthquakes. I will start with theoretical considerations on dynamic pressure.

2. Dynamic pressure in the brittle regime

In two-phase flow, fluid pressure and solid pressure can be different owing to surface tension and matrix compaction (McKenzie, 1984; Bercovici and Ricard, 2003), but under the simplifying assumptions of zero surface energy and constant porosity, these pressures are equal (e.g., Spiegelman and McKenzie, 1987; Faccenda et al., 2009). Fluid flow is driven by buoyancy as well as dynamic pressure gradients, and to enable downward water transport, the effect of dynamic pressure, which is caused by the deformation of the solid phase, should be greater than that of buoyancy. In the limit of static or steady-state faulting, the magnitude of dynamic pressure associated with bending-related (normal) faulting can be estimated by simple force balance, as shown below.

Assuming that the stresses in the x , y , and z directions are the principal stresses and that no strain in the y direction, the stress state appropriate for normal faulting owing to horizontal extension in the x direction may be expressed as (e.g., Turcotte and Schubert, 1982)

$$\sigma_{xx} = -\rho gz + \Delta\sigma_{xx}, \quad (1)$$

$$\sigma_{yy} = -\rho gz + \nu\Delta\sigma_{xx}, \quad (2)$$

$$\sigma_{zz} = -\rho gz, \quad (3)$$

where ρ is density, g is gravitational acceleration, and z is depth, $\Delta\sigma_{xx}$ is tensional deviatoric stress, and ν is Poisson's ratio. The deviatoric stress that can be supported by a fault with dip β is given by

$$\Delta\sigma_{xx} = \frac{2\mu(1-\lambda)\rho gz}{\sin 2\beta + \mu(1-\cos 2\beta)}, \quad (4)$$

where μ is the friction coefficient, and λ is pore fluid pressure normalized by lithostatic pressure (ρgz). Dynamic pressure corresponding to normal faulting may be thus written as

$$p = -\frac{1}{3}(\sigma_{xx} + \sigma_{yy} + \sigma_{zz}) - \rho gz \\ = -\frac{1+\nu}{3} \frac{2\mu(1-\lambda)\rho gz}{\sin 2\beta + \mu(1-\cos 2\beta)}. \quad (5)$$

As shown in Fig. 1a, the dynamic pressure can fully compensate for confining pressure only when the fault dip is very low (~ 10 – 20°), which is much lower than the optimal dip for normal faulting ($\sim 60^\circ$). Outer rise earthquakes with normal faulting exhibit dip angles close to the optimal value (Christensen and Ruff, 1988), indicating that the associated dynamic pressure can reduce confining pressure by $\sim 50\%$ at most. The dynamic pressure is less negative for lower friction coefficient or higher pore fluid pressure, and the case of $\mu = 0.8$, $\lambda = 0$, and $\nu = 0.25$ shown in Fig. 1a is likely to serve as the lower bound. The λ value is ~ 0.3 when pore fluid pressure is hydrostatic, and higher pore fluid pressure acts to further decrease the magnitude of dynamic pressure. Equation (5) holds for all depths as long as brittle deformation takes place, so normal faulting does not reduce confining pressure sufficiently to allow downward water transport.

The above calculation is based on a static or steady-state force balance, but the consideration of a more dynamic situation, e.g., rupture propagation, would not affect the conclusion. The magnitude of any dynamic effect on stress caused by an earthquake can be estimated by dividing the radiated seismic energy by the

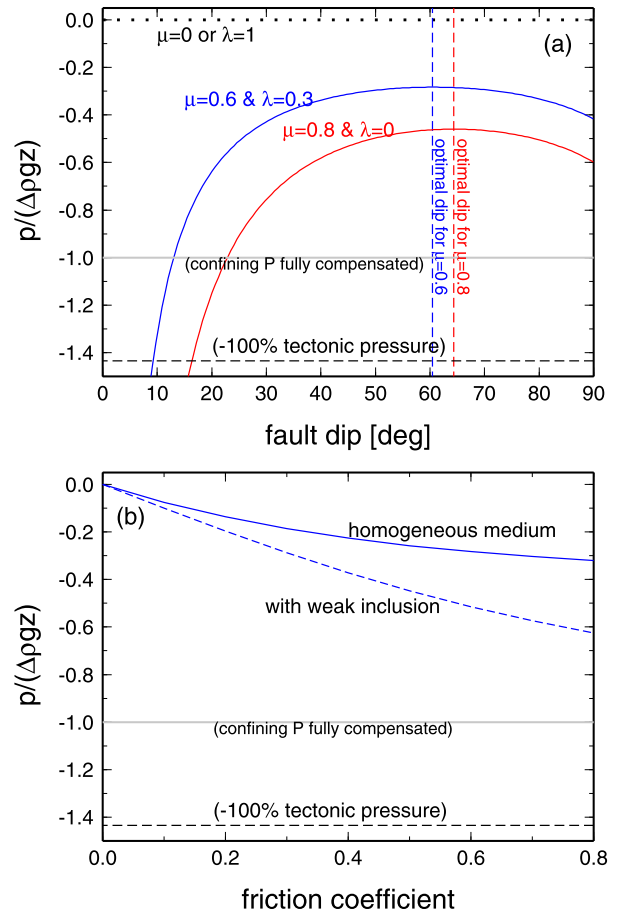


Fig. 1. (a) Dynamic pressure generated by normal faulting as a function of fault dip β , according to equation (5). Pressure is normalized by confining pressure $\Delta\rho gz$ ($= (\rho - \rho_w)gz$), where ρ_w is water density. Red curve denotes the case of $\mu = 0.8$ and $\lambda = 0$, and blue curve the case of $\mu = 0.6$ and $\lambda = 0.3$. In both cases, the Poisson's ratio ν is set to 0.25. Dotted line denotes the case of $\mu = 0$ or $\lambda = 0$. The location of optimal fault dip, corresponding to the minimum deviatoric stress (i.e., $\tan 2\beta = -1/\mu$), is shown by vertical line. The level of dynamic pressure required to fully compensate confining pressure is shown by horizontal gray line, and -100% tectonic pressure, which was somehow achieved in the numerical model of Faccenda et al. (2009), is by horizontal dashed line. (b) Dynamic pressure by normal faulting as a function of friction coefficient, with $\lambda = 0.3$ (hydrostatic), $\nu = 0.25$, and the optimal fault dip. Solid line denotes the case of a homogeneous medium (equation (5)), while dashed line denotes the maximum effect caused by viscosity heterogeneities along the optimally dipped fault (equation (6)). (For interpretation of the references to color in this figure legend, the reader is referred to the web version of this article.)

volume involved. This is the so-called the stress drop, which is on the order of only 1–10 MPa (Shearer, 2009).

The numerical modeling of Faccenda et al. (2009) is based on the visco-elasto-plastic code of Gerya and Yuen (2007), in which brittle deformation is taken into account. It is therefore puzzling that their models exhibit strongly negative dynamic pressure, enough to compensate for lithostatic pressure down to the depth of a few tens of km, along with the formation of normal faults with dip of $\sim 60^\circ$. The 'tectonic' pressure in Faccenda et al. (2009) is defined as deviation from lithostatic pressure, and -100% tectonic pressure seen in their models is equivalent to dynamic pressure entirely canceling lithostatic pressure, which is greater than confining pressure by $\sim 40\%$. The friction coefficient used is in the range of 0.4–0.6, which conforms to the fault dip seen in the models, but the amplitude of dynamic pressure seems too large.

One way to explain the strongly negative pressure of Faccenda et al. (2009) is to assume that a fault zone is inherently weaker than the surrounding rocks; viscosity heterogeneities could dis-

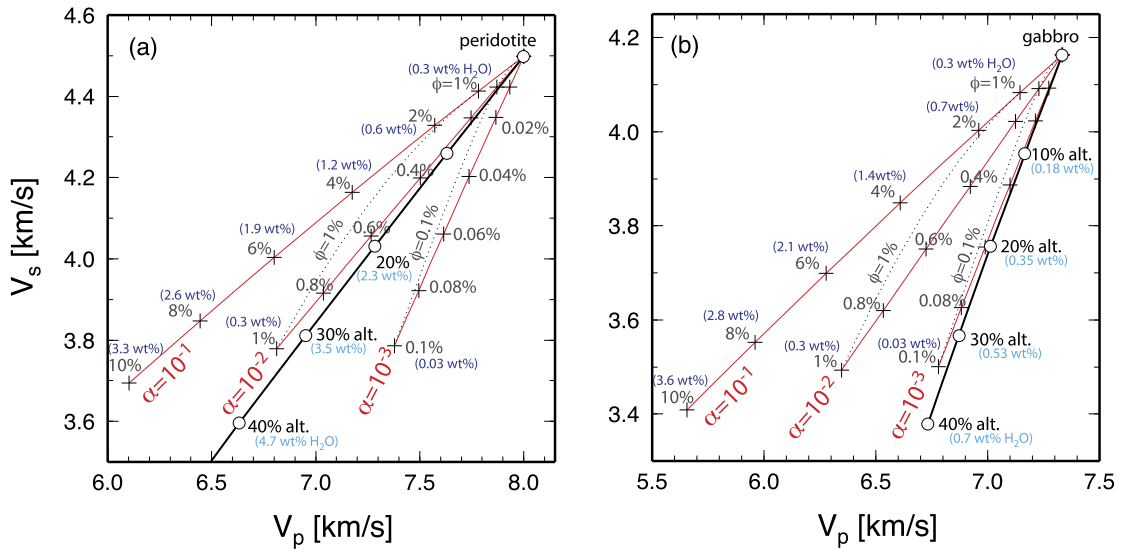


Fig. 2. (a) Effects of serpentinization (solid line with open circles) and crack porosity (red lines with crosses) on the seismic velocities of peridotite. Numbers next to symbols denote the degree of alteration or porosity. For crack porosity, the cases of three different aspect ratios (10^{-1} , 10^{-2} , and 10^{-3}) are shown. Numbers in parentheses are equivalent water contents. Dotted lines connecting different aspect ratios (but with the same porosity) illustrate the effect of varying the aspect ratio. The following properties are assumed: for peridotite, $K = 123.2$ GPa, $G = 67.4$ GPa, and $\rho = 3330$ kg m $^{-3}$; for serpentinite, $K = 40.1$ GPa, $G = 12.4$ GPa, and $\rho = 2460$ kg m $^{-3}$; for sea water, $K = 2.44$ GPa, $G = 0$, and $\rho = 1023$ kg m $^{-3}$; and for air, $K = 0.15$ MPa, $G = 0$, and $\rho = 0$ (air properties are necessary when using the Gassman low-frequency relations). For the effect of crack porosity, effective elastic moduli of dry porous rock were first calculated using the formula of Kuster and Toksöz (1974), and then the Gassman low-frequency relations were applied to obtain effective moduli for fluid saturated porous rock (Mavko et al., 1998). Elastic moduli for peridotite and serpentinite are based on Christensen (2004), and those for seawater are taken from Wilkens et al. (1991). For serpentinite, data for lizardite serpentinites are used here; this is appropriate when the mantle just below the normal oceanic crust near subduction zone is colder than 300 °C. For higher temperatures, antigorite forms instead, and its effect on seismic velocities follows the same trend of that for lizardite; the only difference is the corresponding degree of alteration, and a factor of ~ 2.5 should be multiplied to convert from lizardite values (e.g., V_p of ~ 6.6 km s $^{-1}$ and V_s of ~ 3.6 km s $^{-1}$ corresponds to 40% alteration in case of lizardite, but to 100% alteration in case of antigorite). (b) Effects of alteration and crack porosity on the seismic velocities of gabbro. The following properties are assumed based on Carlson and Miller (2004): for gabbro, $K = 92$ GPa, $G = 52$ GPa, and $\rho = 3000$ kg m $^{-3}$; and for 40% altered gabbro, $K = 87$ GPa, $G = 33$ GPa, and $\rho = 2890$ kg m $^{-3}$. (For interpretation of the references to color in this figure legend, the reader is referred to the web version of this article.)

place pressure locally from the ambient pressure (Moulas et al., 2014), and the theoretical bound of equation (5) could be violated. This possibility can be tested by a bound on the effect of viscosity heterogeneities:

$$p = -\frac{1}{2}(1 - \cos 2\beta)\Delta\sigma_{xx}, \quad (6)$$

which is derived from the analytical solution of Moulas et al. (2014) by taking the limit of zero inclusion viscosity and an infinite aspect ratio. As seen in Fig. 1b, this effect is not strong enough to cancel confining pressure. It thus remains difficult to understand the strongly negative pressure of Faccenda et al. (2009) on a theoretical basis; it may originate in the implementation details of the visco-elasto-plastic code employed in their study, and further investigation is warranted on this matter.

3. Observational constraints

3.1. Active-source seismology

Since the work of Ranero et al. (2003), which suggests the occurrence of bending-related faulting in the top ~ 20 km of the incoming plate at the Middle America trench, a number of active-source seismic studies have followed to quantify the extent of hydration caused by bending (e.g., Ranero and Sallarès, 2004; Grevenmeyer et al., 2007; Contreras-Reyes et al., 2008; Ivandic et al., 2008; Van Avendonk et al., 2011; Lefeldt et al., 2012; Fujie et al., 2013). Seismic tomography models in these studies constrain only the very shallow portion of the mantle, from the top ~ 1 km (e.g., Ranero and Sallarès, 2004) to ~ 10 km (e.g., Van Avendonk et al., 2011). Most of these studies provide estimates only on P -wave velocity structure, and even when S -wave velocity models are available, their coverage of the mantle section is limited to

the top ~ 1 km (Contreras-Reyes et al., 2008) or absent (Fujie et al., 2013). The depth extent of velocity reduction in the mantle is not well constrained, as it is influenced by particular smoothing constraints adopted in tomographic inversion, but it is probably safe to conclude that the top few km of the mantle section is typically characterized by 5–10% reduction in P -wave velocity.

This reduction in the P -wave velocity is usually interpreted as the effect of serpentinization (Christensen, 2004), and $\sim 10\%$ reduction in the P -wave velocity of the mantle section then implies $\sim 20\%$ serpentinization (Fig. 2a), which is equivalent to ~ 2 wt% H $_2$ O. If serpentinization takes place above ~ 300 °C, antigorite forms instead of lizardite, and in such case, the same velocity reduction corresponds to $\sim 50\%$ serpentinization, i.e., ~ 6 wt% H $_2$ O. Some studies (e.g., Ivandic et al., 2008; Lefeldt et al., 2012) also mention the effect of fracture or crack-like porosity, indicating that this estimate of hydration is merely an upper bound, but they tend to dismiss its significance by suggesting that fractures promote hydration. The presence of water-filled fractures or cracks, however, does not necessarily lead to the hydration of surrounding rocks (see Section 3.2), and it is worth considering the effect of crack-like porosity independently from that of serpentinization.

As shown in Fig. 2a, 1% porosity filled with water leads to $\sim 3\%$ reduction in P -wave velocity if the aspect ratio of the porosity is 0.1, whereas the same porosity gives rise to $\sim 15\%$ reduction for the aspect ratio of 10^{-2} . Here the aspect ratio refers to the ratio of the shorter semi-axis over the longer semi-axes of an oblate spheroid, so a smaller aspect ratio means more crack-like. When porosity is more crack-like, velocity reduction is more pronounced, and different aspect ratios lead not only to different sensitivities to porosity, but also to different V_p/V_s ratios. The case with the aspect ratio of 10^{-2} closely follows the V_p/V_s ratio expected for the peridotite-serpentinite mixture. If one observes V_p of 7.0 km s $^{-1}$

and V_S of 3.8 km s^{-1} , for example, it could mean 30% serpentinization or 1% of water-filled fractures. The former corresponds to 3.5 wt% water, and the latter to only 0.3 wt% water. If only P -wave velocity is available, the lower bound for the water content could decrease further by assuming smaller aspect ratios. In the formalism of Kuster and Toksöz (1974), which is used to evaluate the effect of crack-like porosity here, porosity cannot exceed the aspect ratio, and this is why the case of aspect ratio of 10^{-3} shows porosity only up to 0.1%. As Berryman (1980) pointed out, however, this bound on porosity is not rigorous, and the trend of velocity reduction can be extended to much larger porosity. Thus, while it is true that the interpretation with serpentinization provides an upper bound on water content, the merit of this bound is not obvious when the true content can be lower by more than one order of magnitude.

Velocity reduction in the lower-crustal, gabbroic section is also commonly observed in incoming plates (e.g., Ranero and Sallarès, 2004; Van Avendonk et al., 2011; Fujie et al., 2013). The degree of velocity reduction caused by alteration (mostly amphibole with some phyllosilicates; Carlson and Miller, 2004) is more subdued for gabbroic rocks; for example, 30% alteration causes only ~6% drop in the P -wave velocity of gabbro, as opposed to ~12% drop in that of peridotite (Fig. 2a, b). Therefore, even a small velocity reduction in the lower-crustal section could imply substantial alteration, but the amount of water introduced by alteration is ~7 times smaller for gabbro than for peridotite, when compared at the same degree of alteration. The lower-crustal section is thus an unlikely place to store a large amount of water. Nonetheless, it is still important to interpret the lower-crustal velocity correctly. As shown in Fig. 2b, the effect of alteration on the P - and S -wave velocities of gabbro is indistinguishable from that of water-filled porosity with the aspect ratio of 10^{-3} , but the amount of water involved is two orders of magnitude less in the latter. This ambiguity is not limited to the interpretation of the crustal velocity of the incoming plates. The normal oceanic lower-crust has long been known to exhibit V_P of $\sim 7.0 \text{ km s}^{-1}$ (White et al., 1992), whereas the P -wave velocity of unaltered gabbro is $\sim 7.3 \text{ km s}^{-1}$ (Fig. 2b). So the lower-crustal velocity is already reduced by ~4% before arriving at subduction zones. Korenaga et al. (2002) suggested crack porosity as a cause for this velocity reduction, whereas Carlson (2003) proposed alteration as a chief culprit. Based on a theoretical study of thermal stress, Korenaga (2007b) showed that oceanic plates are likely to be pervasively fractured by thermal cracks, so the possible role of crack porosity is hard to discount. Carlson (2003) argued that crack porosity alone should not explain the observed velocity reduction because a network of cracks would serve as a conduit for hydrothermal fluids and cause more alteration. As discussed next, cracks and alteration are not so simply related as commonly believed.

3.2. Note on the rate of hydration through wall rocks

When Ranero et al. (2003) estimated how quickly the mantle could be hydrated (horizontally) from bending-related faults, they used the diffusion speed of water in unfractured serpentine, which was estimated to be $\sim 1 \text{ km Myr}^{-1}$ by Macdonald and Fyfe (1985). At temperatures above 100°C , the rate of serpentinization is geologically rapid, regulated mostly by the rate of water delivery. When a water-filled fracture forms by tension, therefore, how quickly water in the fracture can flow into wall rocks controls the rate of serpentinization. Macdonald and Fyfe (1985) argued that such horizontal water transport would be driven by a pressure difference between hydrostatic pressure (in the crack) and the equilibrium vapor pressure of serpentinization reaction at the reaction interface.

For this transport mechanism to work, the following three conditions must be satisfied: (1) the pressure relevant for the serpentinization reaction is pore fluid pressure, (2) the solid matrix is strong enough to allow the occurrence of sublithostatic pressure within the pore space (i.e., pressure reduction caused by serpentinization can be sustained), and (3) there exists ubiquitous water-filled porosity throughout the serpentinized and unaltered sections. The first condition is probably valid (Dahlen, 1992), and the second condition may be satisfied at low lithostatic pressures. The third condition, however, leads to a circular logic: The unaltered part, to which water needs to be delivered, has to already contain water. The third condition is necessary because the use of the equilibrium vapor pressure in the argument of Macdonald and Fyfe (1985) makes sense only for reaction in a closed system. Even if the third condition is satisfied, such pre-existing porosity in the unaltered section would be quickly reduced by the large volume expansion (~50%) associated with serpentinization. Volume expansion may cause cracking and create new porosity, but the creation of new porosity becomes more difficult at higher pressures, as it needs to compete with the confining pressure. For mantle rocks to be hydrated substantially, therefore, they must have sufficiently high porosity beforehand. Given that residual microscopic porosity tends to decrease with increasing lithostatic pressure, hydration through wall rocks is expected to be more limited at greater depths.

Also, there is one field evidence against the transport mechanism proposed by Macdonald and Fyfe (1985). The essence of their mechanism is that water is sucked up by a very low vapor pressure at the reaction front, which is located inside wall rocks. Normally, fluid within wall rocks is subject to the lithostatic pressure, which acts to expel the fluid out of wall rocks instead of sucking it up, but in the mechanism of Macdonald and Fyfe (1985), the equilibrium vapor pressure nullifies the effect of lithospheric pressure and reverts the sense of water transport. If this mechanism can really work, it should work also for serpentinization in the vertical direction, and it would be difficult to explain why the serpentinized mantle seen at non-magmatic rifted margins (i.e., with no significant crustal layer) such as the Iberian margin is only 5–6 km thick (e.g., Minshull, 2009). With the serpentinization rate as high as 1 km Myr^{-1} , and if the equilibrium vapor pressure can suck up water regardless of confining pressure, the top half of lithosphere (50 km or so), in which serpentine is stable, can easily be 100% serpentinized because such passive margins were all formed a few tens of million years ago. This hypothetical serpentinization assumes an ongoing supply of seawater, and one may question whether such a supply may be limited by ongoing mineralization in fault zones and sediment blanketing. According to Macdonald and Fyfe (1985), however, the mechanism by which water diffuses into peridotites to generate serpentine is the flow of water through defects in the serpentine structure and not through finite microcracks. In other words, whereas microcrack porosity provides water to the edges of the diffusive region, the primary mechanism of hydration is diffusion through what are essentially nanoscale defects. Thus, the flow of water through the bulk of serpentinized fractions would be unaffected by the details of fault zone processes. Also, because sediments are usually characterized with high porosities (>10%; e.g., Nafe and Drake, 1957), sediment blanketing is unlikely to hinder downward water transport along a huge pressure gradient caused by the low equilibrium vapor pressure at the reaction front. Therefore, the reason why only top few kilometers is serpentinized in those non-magmatic margins is most likely that, at the time of continental breakup, only the shallow part of the mantle was cold enough to be brittle, thereby pervasively fractured by rifting, and at relatively low confining pressures, porosity due to such fractures could be high.

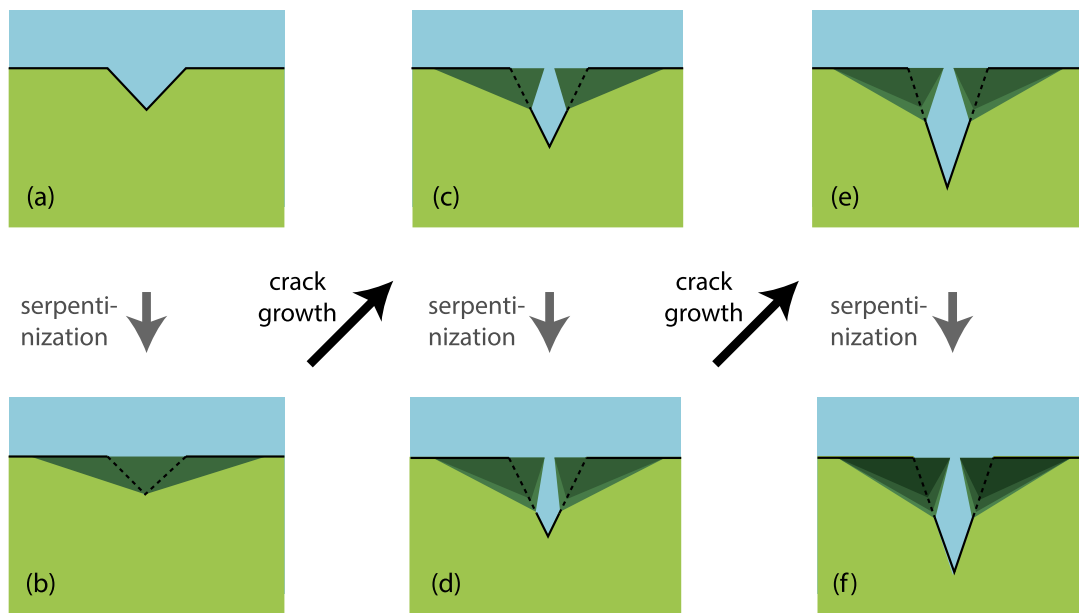


Fig. 3. Schematic illustration for how thermal cracking may proceed with the serpentinization of wall rocks. When cracks are shallow (a), pore water in the crack would be largely consumed by serpentinization, and the crack space could be filled by the volume expansion associated with the reaction (b). Continued crack growth would keep the serpentinized lid open and introduce more pore water (c, e). Serpentinization would follow, but because of higher lithostatic pressure involved, the serpentinization of wall rocks would be less efficient (d, f). Confining pressure acting on wall rocks may exceed their tensional strength, so wall rocks could eventually collapse by normal faulting if they contain optimally oriented weaknesses. See text for discussion.

3.3. On the state of oceanic lithosphere before entering a subduction zone

According to the numerical modeling of Korenaga (2007b), oceanic plates may gradually be fractured rather pervasively by thermal cracking. Bending-related faulting would take place on top of this process, so it is important to consider the consequence of thermal cracking to better understand a reference state.

Because deep cracks do not release thermal stress at shallow depths efficiently, the most likely situation would be the cascade crack system in which narrowly-spaced shallow cracks and widely-spaced deep cracks coexist. Deeper cracks would grow as the plate cools; using the rheology of oceanic plates, substantial thermal stress can be expected at temperatures lower than $\sim 600^\circ\text{C}$. These thermal cracks are tension cracks formed by net volume contraction, so unlike normal faults, downward water transport is guaranteed as long as cracks are open. For a 100-Ma oceanic plate, 20–30 km deep cracks are expected to form with an interval of a few tens of kilometers, each crack having average opening of ~ 50 m (coexisting shallower cracks would form with narrower intervals and smaller openings) (Korenaga, 2007b). Because of the difficulty of horizontal water transport discussed in the previous section, water in deep cracks would not be easily consumed by serpentinization (Fig. 3). The spatially averaged porosity created by thermal cracking is estimated to be 0.1–0.2% (Korenaga, 2007b). Crack porosity can of course be locally higher than this average value.

These vertical cracks are hard to be imaged seismically. Also, the wall rocks of thermal cracks are subject to large confining pressures (~ 450 MPa at the depth of 20 km), so open cracks could eventually collapse by normal faulting, and the above estimate on average porosity serves as an upper bound. This collapse by normal faulting would release any residual (extensional) thermal stress and put oceanic plates into the compressional stress state, most likely due to ridge push (Dahlen, 1981), as indicated by the focal mechanisms of intra-plate earthquakes (Wiens and Stein, 1983). The presence of thermal cracks, however, lowers the effective thermal expansivity of oceanic plates (Korenaga, 2007a), and

the apparent thermal expansivity estimated from the age–depth relationship of normal seafloor is close to that predicted by thermal cracking (Korenaga and Korenaga, 2008). This implies that the collapse of wall rocks may be inefficient in reducing the porosity, or the collapse itself does not always take place. Confining pressure is very close to the tensional yield strength, so if wall rocks do not contain optimally oriented weaknesses, they could sustain confining pressure. Alternatively, the collapse of wall rocks could lead to the enhanced serpentinization of oceanic plates, and if water in open cracks were entirely consumed by serpentinization, it would also lower the effective thermal expansivity of oceanic plates (Korenaga, 2007a). The fate of water introduced by thermal cracking thus hinges on the subtle balance between confining pressure and tensional yield strength. Some thermal cracks could trap water as depicted in Fig. 3, while others might be completely filled with serpentine. An intermediate situation, in which wall-rock collapse results in partial serpentinization as well as trapped water, would also be possible.

Oceanic plates are thus expected to be pervasively fractured by thermal cracks and normal faults to various degrees, even before arriving at subduction zones. Bending-related normal faulting is very likely to further promote the collapse of wall rocks, enhancing the background porosity introduced by thermal cracking. The seismic velocity anomalies observed in the shallow mantle section of incoming plates (Section 3.1) may be explained by such an increase in porosity, and as shown by Fig. 2, a slight increase in (crack-like) porosity can have a dramatic effect on seismic velocities.

3.4. Other geophysical observations

Electrical resistivity measurements can provide independent constraints on the volume of pore fluid in the incoming plates, and there is one marine controlled-source electromagnetic survey focused on crustal and uppermost mantle structure conducted at a subduction zone (Naif et al., 2015). Based on a 220-km-long transect across the Middle America Trench, Naif et al. (2015) estimated how plate bending affects the porosity profile through the crust and down to the top ~ 1 km of the mantle. Their inversion results

suggest that the porosity of the lower crust exhibits about a two-fold increase from the pre-bending value of $\sim 0.7\%$, whereas that of the uppermost mantle does not seem to be affected by bending, with the value of $\sim 0.4\text{--}0.5\%$ throughout the transect. Because of uncertainties associated with the conversion from electrical resistivity to porosity, these porosities are better regarded as an upper bound (Naif et al., 2015). Even a fraction of these porosities is sufficient to explain the observed velocity reduction in the incoming plates (Fig. 2), implying a diminishing role of alteration.

In addition to marine geophysical surveys, there have also been efforts to utilize teleseismic data. Faccenda et al. (2008) argued that the delay time of SKS splitting at subduction zones (typically around 1–2 s) can be explained by the substantial serpentinization of incoming plates, which originates in bending-related faulting. Because SKS phases sample not only the subducting slab but also the wedge mantle and the sub-slab mantle, however, the interpretation of the splitting delay time is non-unique (e.g., Katayama et al., 2009; Long, 2013). By analyzing earthquakes from the well-defined double seismic zone beneath northeastern Japan, Huang et al. (2011) were able to isolate the effect of the subducting slab, and their results suggest that the delay time due to the subducting slab is only ~ 0.1 s. Recently, Garth and Rietbrock (2014) proposed that the top 40 km of the subducting slab may be up to $\sim 30\%$ serpentinized, based on the analysis of *P*-wave arrivals from intermediate-depth earthquakes that took place within the subducting slab beneath Hokkaido, Japan. Their inference assumes, however, that the normal oceanic plate before subduction is free of any seismic heterogeneities. The study of *Po/So* phases (i.e., suboceanic *Pn/Sn* phases) indicates that oceanic plates contain a variety of small-scale heterogeneity, the strength of which appears to be regionally variable (Kennett et al., 2014), so properly extracting the effect of plate bending seems challenging.

4. Origin of intermediate-depth earthquakes

The notion of the deep hydration of incoming plates by faults associated with outer-rise earthquakes was put forward by Peacock (2001), to explain lower-plane earthquakes in the double seismic zone by dehydration embrittlement. Seno and Yamanaka (1996) were the first to suggest dehydration embrittlement as the cause of lower-plane earthquakes, but they considered that such deep hydration by outer-rise earthquakes was unlikely and instead suggested that some incoming plates happened to have been hydrated from below by the migration of hydrous melts derived from the impingement of a plume. Their arguments against deep hydration by bending-related normal faulting are detailed by Yamasaki and Seno (2003): (1) the mechanism of deep outer-rise earthquakes is usually compressional not tensional, (2) lower-plane earthquakes are more sporadic than upper-plane earthquakes, and (3) the occurrence of the double seismic zone is limited to only a few subduction zones. Since then, Brudzinski et al. (2007) have shown that the double seismic zone is globally observed, making the plume-induced hydrous melt hypothesis unlikely. Also, thermal cracking could introduce water down to the isotherm of $\sim 600^\circ\text{C}$, so the mechanism of outer-rise earthquakes becomes irrelevant. While bending-related faulting may not hydrate incoming plates deeply, therefore, lower-plane earthquakes could still be caused by dehydration embrittlement.

Lower-plane earthquakes may also be caused by a process that does not involve any water, such as the shear heating mechanism of Kelemen and Hirth (2007), in which highly localized viscous creep takes place in pre-existing fine-grained shear zones. The attractive feature of this mechanism is that the onset of such instability is limited in the temperature range of $600\text{--}800^\circ\text{C}$, in which lower-plane earthquakes are considered to occur. The olivine flow law assumed by Kelemen and Hirth (2007) is, however, subject

to large uncertainty, particularly regarding pressure dependency (Korenaga and Karato, 2008), so it is unclear whether shear instability could account for all of lower-plane earthquakes, which take place over the wide depth range of 50–200 km (e.g., Yamasaki and Seno, 2003; Brudzinski et al., 2007). Moreover, the instability requires pre-existing fine-grained shear zones. Kelemen and Hirth (2007) suggested that oceanic transforms and outer-rise faults may create such zones of weakness, but then it would become difficult to explain the sporadic nature of lower-plane earthquakes. As mentioned above, Yamasaki and Seno (2003) considered that deep mantle hydration by bending-related normal faulting, which has a spacing of $\sim 2\text{--}3$ km, was unlikely because it should lead to a much denser distribution of lower-plane earthquakes than observed (Igarashi et al., 2001).

The sparseness (or less uniform distribution) of lower-plane earthquakes, in comparison to upper-plane earthquakes, is not an artifact due to insufficient observations, at least for the double seismic zone beneath Japan. A very dense seismic network covers the Japanese Islands at station intervals of 15–20 km, and Kita et al. (2010a) relocated $\sim 98,000$ earthquakes that occurred at depths of 20–300 km beneath northeastern Japan during the period from June 2002 to December 2007. Their spatial distribution is shown in Fig. 4. It is now possible to detect very small intra-plate earthquakes ($M_j > 1.2$ (Kita, 2009); M_j is the local magnitude scale used by Japan Meteorological Agency and, for intermediate-depth earthquakes, it is similar to M_W), and the patchy distribution of lower-plane events is indisputable. It is unclear how such a distribution could result from densely spaced normal faults. Recently, Shillington et al. (2015) suggested pre-existing plate fabric could influence on bending faulting and plate hydration, based on seismic observations in the Alaska Peninsula subduction zone, but this possibility does not explain the sparseness of the lower-plane earthquakes beneath northeastern Japan because upper-plane earthquakes are densely distributed regardless of the ridge fabric of the subducting plate (Nakanishi et al., 1992). I suggest that the cascade crack system expected for thermal cracking may provide a natural explanation, because deeper cracks are more widely spaced. It is still difficult to theoretically predict the planform of thermal cracking, but inferring from natural examples such as columnar joints, a hexagonal pattern may be ideal (e.g., Lister, 1974), if the influence of tectonic stress is minimal. It is also well known that, for two-dimensional elastic deformation, hexagonal symmetry reduces to isotropy (Landau and Lifshitz, 1970). Such a hexagonal crack system filled with water or serpentine releases water as it exceeds the stability zone of hydrous minerals, and the released water is likely to migrate upward, due to its own buoyancy, and react with unaltered peridotites along the dehydration front (Fig. 5). If lower-plane earthquakes take place due to dehydration embrittlement, therefore, their spatial distribution may resemble a smeared version of the hexagonal lattice.

With the assumption of dehydration embrittlement, it is possible to estimate the minimum degree of steady-state mantle hydration needed for the very occurrence of lower-plane earthquakes. First, the length of the subduction zone responsible for intra-plane events in Fig. 4 is approximately 1100 km. With the subduction velocity of 8 cm yr^{-1} and the depth range of 23–40 km for lower-plane events, the input volume flux of the relevant mantle is $\sim 1.5 \times 10^9\text{ m}^3\text{ yr}^{-1}$. Second, the frequency of lower-plane earthquakes with $M_W \geq 3.0$ in this region is ~ 40 per year (Kita, 2009). The frequency–magnitude distribution of earthquakes generally exhibits the following power-law relation (e.g., Shearer, 2009):

$$\log_{10} N = a - bM, \quad (7)$$

where N is the number of events with magnitude greater than or equal to M , a is the total number of earthquakes, and b measures

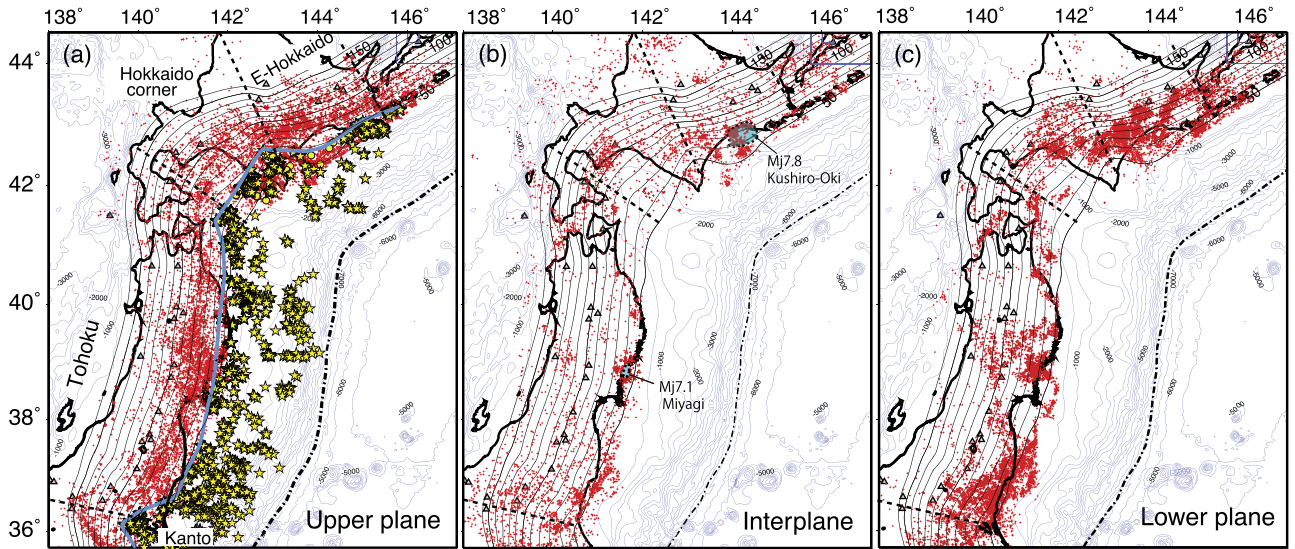


Fig. 4. Epicenter distributions of earthquakes (a) in the upper plane, (b) in the interplane, and (c) in the lower plane, of the double seismic zone beneath northeastern Japan (all shown in red dots). Upper-plane earthquakes are those which occur in the top 10 km of the subducting plate, and lower-plane events are between ~23 km and ~40 km from the plate interface. Gray triangles and black contours show, respectively, active volcanoes and the depth of the plate interface. A thick blue line shows the downdip limit of inter-plate earthquakes. Blue thin lines are bathymetric contours with a 500 m interval. Yellow stars and yellow circles denote the epicenters of small repeating earthquakes and low-angle thrust type events, respectively. After [Kita et al. \(2010b\)](#). (For interpretation of the references to color in this figure legend, the reader is referred to the web version of this article.)

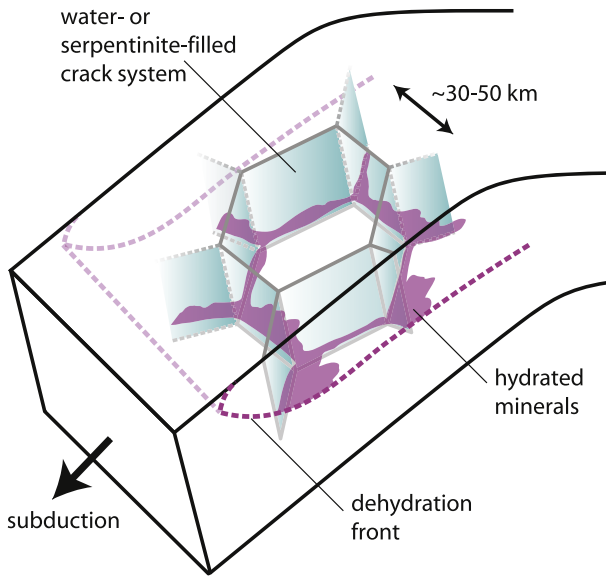


Fig. 5. Schematic illustration for the role of thermal cracks in the generation of lower-plane earthquakes in the double seismic zone. Thermal cracking is likely to result in a cascade crack system with variable crack lengths, and only deepest cracks are depicted here. Those deep cracks are filled with seawater or serpentine, and when they cross the dehydration front (dashed line), released water would migrate upward, probably in the form of dike propagation, and react with unaltered peridotites. Dehydration embrittlement in such a smeared hexagonal lattice (shown in purple) may explain the spatial distribution of lower-plane earthquakes. (For interpretation of the references to color in this figure legend, the reader is referred to the web version of this article.)

the relative number of large quakes compared to small quakes. The b -value for lower-plane earthquakes under northeastern Japan is ~0.8 ([Kita, 2009](#)), so the frequency for $M_W \geq 5.0$ events, for example, is ~1 per year.

Third, the linear dimension of a rupture area, r , may be estimated from the seismic moment, M_0 , using the formula for a circular fault ([Shearer, 2009](#)):

$$M_0 = k\Delta\sigma r^3, \quad (8)$$

where $k = 16/7$, and $\Delta\sigma$ is the stress drop. At the same time, the definition of the seismic moment is

$$M_0 = \mu AD, \quad (9)$$

where μ is shear modulus, A is the area of rupture along a fault, and D is the average displacement. For the case of a circular fault, $A = \pi r^2$. The volume of hydrous minerals that contains the fault may be estimated as $\pi r^2 h$, where h is the thickness of the hydrous layer. The volume most relevant to the present discussion is, however, the volume of hydrous minerals that are expended by slip along a fault; I am trying to relate the frequency of earthquakes with the incoming flux of hydrous minerals, which is equivalent to the outgoing flux of hydrous minerals under the steady-state assumption. The volume of hydrous minerals expended by slip along a fault is $2rhD$. For lower-plate earthquakes, the stress drop is ~20 MPa ([Kita and Katsumata, 2015](#)), so for an event with M_W of 5.0 (or M_0 of $\sim 3.5 \times 10^{16}$ Nm), for example, the rupture radius r is ~1 km. Using the peridotite value of 70 GPa for μ , the displacement D is ~20 cm. How thick the layer should be to generate an earthquake by dehydration embrittlement is not known. The roughness of a fault surface would provide a bare minimum estimate, which is vanishingly thin for exposed faults (e.g., [Candela et al., 2012](#)). As an alternative, more conservative estimate, one may consider the thickness of a fault zone made of gouge and breccia, which exhibit a linear relationship with the displacement, $h \sim D$ (e.g., [Childs et al., 2009](#); [Faulkner et al., 2010](#)). With this scaling, a fault zone thickens as displacement continues. Though it is not known how many times a single fault plane is reused in dehydration embrittlement, the thickness of fault rock (or fault core), along which slip takes place, is about two orders of magnitude smaller than that of fault zone ([Childs et al., 2009](#)), so the above simple linear scaling should serve as a reasonable upper bound. The expended volume would then be just ~70 m³ for an event with M_W of 5.0, and it may be expressed as a function of moment magnitude as

$$\begin{aligned} v(M_W) &\sim \frac{2k\Delta\sigma}{(\mu\pi)^2} M_0(M_W) \\ &\sim \frac{2k\Delta\sigma}{(\mu\pi)^2} 10^{\frac{3}{2}M_W + 9.05}. \end{aligned} \quad (10)$$

The total expended volume flux can be estimated by integrating over magnitude as

$$F_{EV} = \int_{-\infty}^{M_{\max}} n(M_W) v(M_W) dM_W, \quad (11)$$

where M_{\max} is the maximum magnitude, and $n(M_W)$ is the (differential) frequency of events with magnitudes between $M_W - dM_W$ and M_W , i.e., $b10^{a-bM_W} \ln 10$. Using equation (10), the total flux is evaluated as

$$F_{EV} \sim \frac{2k\Delta\sigma}{(\mu\pi)^2} \frac{b}{\frac{3}{2} - b} 10^{9.05+a+(\frac{3}{2}-b)M_{\max}} \quad (12)$$

$$\sim 1 \times 10^4 \text{ m}^3 \text{ yr}^{-1} \cdot \left(\frac{\Delta\sigma}{20 \text{ MPa}} \right) \cdot \left(\frac{70 \text{ GPa}}{\mu} \right)^2. \quad (13)$$

In equation (13), $a = 4.0$, $b = 0.8$, and the maximum M_W is set to 8.0 (the largest lower-plane event in this region has been the 1993 Kushiro-oki earthquake with $M_W = 7.6$). Larger earthquakes expend more volumes, so the total volume will increase with using a higher maximum magnitude or a lower b -value. For example, using the maximum M_W of 9.0 or b of 0.7, F_{EV} would become $\sim 4 \times 10^4 \text{ m}^3 \text{ yr}^{-1}$. The volume flux could also be raised by assuming lower μ ; the shear modulus of serpentinite is, for example, $\sim 12 \text{ GPa}$. The shear modulus used in the seismic moment is, however, that of host rocks that are responsible for elastic strain. The assumed peridotite value in equation (13) is thus appropriate at least for large earthquakes, which occupy the dominant fraction of the total volume flux.

Finally, dividing this expended volume flux ($1 \times 10^4 \text{ m}^3 \text{ yr}^{-1}$) by the input volume flux ($1.5 \times 10^9 \text{ m}^3 \text{ yr}^{-1}$), the minimum volume fraction of hydrous minerals required to explain lower-plane earthquakes by dehydration embrittlement may be estimated to be $\sim 7 \times 10^{-6}$, which is equivalent to $\sim 0.8 \text{ wt. ppm H}_2\text{O}$ or $\sim 2 \times 10^{-4}\%$ of pore fluid. These estimates can be raised by assuming greater layer thickness. The average porosity expected from thermal crack (0.1–0.2%), for example, allows the layer to be thicker than the displacement by three orders of magnitude, i.e., $h \sim 10^3 D$. At the same time, however, water released by dehydration embrittlement could re-enter the dehydration front by upward migration and be reused (Fig. 5), suggesting that an even lower volume fraction of hydrous minerals is permissible.

Based on the detection of a metastable olivine wedge in the subducting slab, Kawakatsu and Yoshioka (2011) argued that an insignificant amount of water (less than 100 wt. ppm) should be present in the slab mantle at least at depths greater than $\sim 400 \text{ km}$. If the fault zone thickness for dehydration embrittlement follows the scaling of shallow, regular earthquakes, the mantle water content could be as low as 1 wt. ppm. Even if the fault zone thickness is greater than the assumed scaling, the distribution of water would be highly localized if thermal cracking is chiefly responsible for the introduction of water, and the bulk of the slab mantle could remain dry (Fig. 5). The observation of the metastable olivine wedge is, therefore, not necessarily inconsistent with the dehydration embrittlement mechanism of lower-plane earthquakes.

5. Conclusion

Whereas it is clear that incoming plates at trenches are often heavily faulted by bending, there is no unambiguous evidence for deep mantle hydration by such bending-related faults, and there is no compelling theoretical reason to expect it, either. Faulting would produce (or enhance) water-filled crack-like porosity, which is sufficient to explain seismic velocity anomalies observed in the

shallow mantle section of incoming plates, without invoking substantial bulk hydration. Hydrating wall rocks around faults requires to keep sucking seawater down, but dynamic pressure associated with normal faulting appears to be too weak to compete with confining pressure, which acts to prevent such deep infiltration of water. Most of water in crack-like porosity would remain unconsumed by hydration because the hydration of wall rocks through lateral water transport is likely to be limited by the confining pressure.

Whereas bending-related faulting takes place only upon subduction, thermal cracking can take place continuously as oceanic plates cool, and it may gradually introduce seawater deep into the mantle, potentially down to the isotherm of $\sim 600 \text{ }^\circ\text{C}$ (e.g., $\sim 30 \text{ km}$ deep for a 100 Myr-old plate). The spatially averaged porosity generated by thermal cracking is 0.1–0.2%, and combined with the present-day subduction rate, the mantle contribution to the global water flux at subduction zones would be $\sim 0.9\text{--}1.8 \times 10^{14} \text{ g yr}^{-1}$ (Korenaga, 2007b). This estimate is a lower bound because processes other than thermal cracking, e.g., plate bending, may introduce additional water, but the occurrence of the double seismic zone, even if it is caused by dehydration embrittlement, does not demand any addition.

Acknowledgements

This work was motivated by discussion with Hitoshi Kawakatsu and was supported in part by a visiting professorship at the Earthquake Research Institute of University of Tokyo. The manuscript also benefited from discussions with Saeko Kita, Satoshi Ide, Jay Ague, Evangelos Moulas, and David Bercovici. The author thanks the editor Bruce Buffett, two anonymous reviewers, and Tim Minshull for constructive comments.

References

- Bercovici, D., Ricard, Y., 2003. Energetics of a two-phase model of lithospheric damage, shear localization and plate-boundary formation. *Geophys. J. Int.* 152, 581–596.
- Berryman, J.G., 1980. Long-wavelength propagation in composite elastic media, II, ellipsoidal inclusions. *J. Acoust. Soc. Am.* 68, 1820–1831.
- Brudzinski, M.R., Thurber, C.H., Hacker, B.R., Engdahl, E.R., 2007. Global prevalence of double Benioff zones. *Science* 316, 1472–1474.
- Candela, T., Renard, F., Klinger, Y., Mair, K., Schmittbuhl, J., Brodsky, E.E., 2012. Roughness of fault surfaces over nine decades of length scales. *J. Geophys. Res., Solid Earth* 117, B08409. <http://dx.doi.org/10.1029/2011JB009041>.
- Carlson, R.L., 2003. Bound water content of the lower oceanic crust estimated from modal analyses and seismic velocities of oceanic diabase and gabbro. *Geophys. Res. Lett.* 30, 2142. <http://dx.doi.org/10.1029/2003GL018213>.
- Carlson, R.L., Miller, D.J., 2004. Influence of pressure and mineralogy on seismic velocities in oceanic gabbros: implications for the composition and state of the lower oceanic crust. *J. Geophys. Res.* 109, B09205. <http://dx.doi.org/10.1029/2003JB002699>.
- Childs, C., Manzocchi, T., Walsh, J.J., Bonson, C.G., Nicol, A., Schöpfer, M.P.J., 2009. A geometric model of fault zone and fault rock thickness variations. *J. Struct. Geol.* 31, 117–127.
- Christensen, D.H., Ruff, L.J., 1988. Seismic coupling and outer rise earthquakes. *J. Geophys. Res.* 93, 13421–13444.
- Christensen, N.I., 2004. Serpentinites, peridotites, and seismology. *Int. Geol. Rev.* 46, 795–816.
- Contreras-Reyes, E., Grevenmeyer, I., Flueh, E.R., Scherwath, M., Bialas, J., 2008. Effect of trench-outer rise bending-related faulting on seismic Poisson's ratio and mantle anisotropy: a case study offshore of Southern Central Chile. *Geophys. J. Int.* 173, 142–156.
- Dahlen, F.A., 1981. Isostasy and the ambient state of stress in the oceanic lithosphere. *J. Geophys. Res.* 86, 7801–7807.
- Dahlen, F.A., 1992. Metamorphism of nonhydrostatically stressed rocks. *Am. J. Sci.* 292, 184–198.
- Faccenda, M., Burlini, L., Gerya, T.V., Mainprice, D., 2008. Fault-induced seismic anisotropy by hydration in subducting oceanic plates. *Nature* 455, 1097–1100.
- Faccenda, M., Gerya, T.V., Burlini, L., 2009. Deep slab hydration induced by bending-related variations in tectonic pressure. *Nat. Geosci.* 2, 790–793.
- Faulkner, D.R., Jackson, C.A.L., Lunn, R.J., Schlische, R.W., Shipton, Z.K., Wibberley, C.A.J., Withjack, M.O., 2010. A review of recent developments concerning the

- structure, mechanics, and fluid flow properties of fault zones. *J. Struct. Geol.* 32, 1557–1575.
- Fujie, G., Kodaira, S., Yamashita, M., Sato, T., Takahashi, T., Takahashi, N., 2013. Systematic changes in the incoming plate structure at the Kuril trench. *Geophys. Res. Lett.* 40, 88–93. <http://dx.doi.org/10.1029/2012GL054340>.
- Garth, T., Rietbrock, A., 2014. Order of magnitude increase in subducted H₂O due to hydrated normal faults within the Wadati–Benioff zone. *Geology* 42, 207–210.
- Gerya, T.V., Yuen, D.A., 2007. Robust characteristic method for modelling multiphase visco-elasto-plastic thermo-mechanical problems. *Phys. Earth Planet. Inter.* 163, 83–105.
- Grevemeyer, I., Ranero, C.R., Flueh, E.R., Kläschen, D., Bialas, J., 2007. Passive and active seismological study of bending-related faulting and mantle serpentinization at the Middle America trench. *Earth Planet. Sci. Lett.* 258, 528–542.
- Huang, Z., Zhao, D., Wang, L., 2011. Shear wave anisotropy in the crust, mantle wedge, and subducting Pacific slab under northeast Japan. *Geochem. Geophys. Geosyst.* 12, Q01002. <http://dx.doi.org/10.1029/2010GC003343>.
- Igarashi, T., Matsuzawa, T., Umino, N., Hasegawa, A., 2001. Spatial distribution of focal mechanisms for interplate and intraplate earthquakes associated with the subducting Pacific plate beneath the northeastern Japan arc: a triple-planed deep seismic zone. *J. Geophys. Res.* 106, 2177–2191.
- Ivandić, M., Grevemeyer, I., Berthot, A., Flueh, E.R., McIntosh, K., 2008. Impact of bending related faulting on the seismic properties of the incoming oceanic plate offshore of Nicaragua. *J. Geophys. Res.* 113, B05410. <http://dx.doi.org/10.1029/2007JB005291>.
- Katayama, I., Kirauchi, K., Michibayashi, K., Ando, J., 2009. Trench-parallel anisotropy produced by serpentine deformation in the hydrated mantle wedge. *Nature* 461, 1114–1117.
- Kawakatsu, H., Yoshioka, S., 2011. Metastable olivine wedge and deep dry cold slab beneath southwest Japan. *Earth Planet. Sci. Lett.* 303, 1–10.
- Kelemen, P.B., Hirth, G., 2007. A periodic shear-heating mechanism for intermediate-depth earthquakes in the mantle. *Nature* 446, 787–790.
- Kennett, B.L.N., Furumura, T., Zhao, Y., 2014. High-frequency *Po/S_o* guided waves in the oceanic lithosphere: II – heterogeneity and attenuation. *Geophys. J. Int.* 199, 614–630.
- Kita, S., 2009. Study for Understanding Generation Mechanisms of Intermediate-Depth Intraslab Earthquakes Beneath Hokkaido and Tohoku, Northeastern Japan. Ph.D. thesis. Tohoku Univ.
- Kita, S., Katsumata, K., 2015. Stress drops for intermediate-depth intraslab earthquakes beneath Hokkaido, northern Japan: differences between the subducting oceanic crust and mantle events. *Geochem. Geophys. Geosyst.* 16, 552–562. <http://dx.doi.org/10.1002/2014GC005603>.
- Kita, S., Okada, T., Hasegawa, A., Nakajima, J., Matsuzawa, T., 2010a. Anomalous deepening of a seismic belt in the upper-plane of the double seismic zone in the Pacific slab beneath the Hokkaido corner: possible evidence for thermal shielding caused by subducted forearc crust materials. *Earth Planet. Sci. Lett.* 290, 415–426.
- Kita, S., Okada, T., Hasegawa, A., Nakajima, J., Matsuzawa, T., 2010b. Existence of interplane earthquakes and neutral stress boundary between the upper and lower planes of the double seismic zone beneath Tohoku and Hokkaido, northeastern Japan. *Tectonophysics* 496, 68–82.
- Korenaga, J., 2007a. Effective thermal expansivity of Maxwellian oceanic lithosphere. *Earth Planet. Sci. Lett.* 257, 343–349.
- Korenaga, J., 2007b. Thermal cracking and the deep hydration of oceanic lithosphere: a key to the generation of plate tectonics? *J. Geophys. Res.* 112, B05408. <http://dx.doi.org/10.1029/2006JB004502>.
- Korenaga, J., Karato, S., 2008. A new analysis of experimental data on olivine rheology. *J. Geophys. Res.* 113, B02403. <http://dx.doi.org/10.1029/2007JB005100>.
- Korenaga, J., Kelemen, P.B., Holbrook, W.S., 2002. Methods for resolving the origin of large igneous provinces from crustal seismology. *J. Geophys. Res.* 107 (B9), 2178. <http://dx.doi.org/10.1029/2001JB001030>.
- Korenaga, T., Korenaga, J., 2008. Subsidence of normal oceanic lithosphere, apparent thermal expansivity, and seafloor flattening. *Earth Planet. Sci. Lett.* 268, 41–51.
- Kuster, G.T., Toksöz, M.N., 1974. Velocity and attenuation of seismic waves in two-phase media, part I, theoretical formulations. *Geophysics* 39, 587–606.
- Landau, L.D., Lifshitz, E.M., 1970. *Theory of Elasticity*. Pergamon.
- Lefeldt, M., Ranero, C.R., Grevemeyer, I., 2012. Seismic evidence of tectonic control on the depth of water influx into incoming oceanic plates at subduction trenches. *Geochem. Geophys. Geosyst.* 13, Q05013. <http://dx.doi.org/10.1029/2012GC004043>.
- Lister, C.R.B., 1974. On the penetration of water into hot rock. *Geophys. J. R. Astron. Soc.* 39, 465–509.
- Long, M.D., 2013. Constraints on subduction geodynamics from seismic anisotropy. *Rev. Geophys.* 51, 76–112.
- Macdonald, A.H., Fyfe, W.S., 1985. Rate of serpentinization in seafloor environments. *Tectonophysics* 116, 123–135.
- Main, I.G., Bell, A.F., Meredith, P.G., Geiger, S., Touati, S., 2012. The dilatancy-diffusion hypothesis and earthquake predictability. In: Healy, D., Butler, R.W.H., Shipton, Z.K., Ribson, R.H. (Eds.), *Faulting, Fracturing and Igneous Intrusion in the Earth's Crust*. Geological Society, pp. 215–230.
- Mavko, G., Mukerji, T., Dvorkin, J., 1998. *The Rock Physics Handbook*. Cambridge Univ. Press, New York.
- McCaig, A.M., 1988. Deep fluid circulation in fault zones. *Geology* 16, 867–870.
- McKenzie, D., 1984. The generation and compaction of partially molten rock. *J. Petrol.* 25, 713–765.
- Minshull, T.A., 2009. Geophysical characterisation of the ocean–continent transition at magma-poor rifted margins. *C. R. Géosci.* 341, 382–393.
- Moulas, E., Burg, J.-P., Podladchikov, Y., 2014. Stress field associated with elliptical inclusions in a deforming matrix: mathematical model and implications for tectonic overpressure in the lithosphere. *Tectonophysics* 631, 37–49.
- Nafe, J.E., Drake, C.L., 1957. Variation with depth in shallow and deep water marine sediments of porosity, density and the velocities of compressional and shear waves. *Geophysics* 22, 523–552.
- Naif, S., Key, K., Constable, S., Evans, R.L., 2015. Water-rich bending faults at the Middle America Trench. *Geochem. Geophys. Geosyst.* 16. <http://dx.doi.org/10.1002/2015GC005927>.
- Nakanishi, M., Tamaki, K., Kobayashi, K., 1992. Magnetic anomaly lineations from Late Jurassic to Early Cretaceous in the west-central Pacific Ocean. *Geophys. J. Int.* 109, 701–719.
- Peacock, S.M., 2001. Are the lower planes of double seismic zones caused by serpentine dehydration in subducting oceanic mantle? *Geology* 29, 299–302.
- Ranero, C.R., Morgan, J.P., McIntosh, K., Reichert, C., 2003. Bending-related faulting and mantle serpentinization at the Middle America trench. *Nature* 425, 367–373.
- Ranero, C.R., Sallarès, V., 2004. Geophysical evidence for hydration of the crust and mantle of the Nazca plate during bending at the north Chile trench. *Geology* 32, 549–552.
- Rüpke, L.H., Phipps Morgan, J., Hort, M., Connolly, J.A.D., 2004. Serpentine and the subduction zone water cycle. *Earth Planet. Sci. Lett.* 223, 17–34.
- Scholz, C.H., Sykes, L.R., Aggarwal, Y.P., 1973. Earthquake prediction – a physical basis. *Science* 181, 803–810.
- Seno, T., Yamanaka, Y., 1996. Double seismic zones, compressional deep trench-outer rise events, and superplumes. In: Bebout, G.E., Scholl, D.W., Kirby, S.H., Platt, J.P. (Eds.), *Subduction: Top to Bottom*. American Geophysical Union, Washington, DC, pp. 347–355.
- Shearer, P.M., 2009. *Introduction to Seismology*. Cambridge Univ. Press.
- Shillington, D.J., Becel, A., Nedimovic, M.R., Kuehn, H., Webb, S.C., Abers, G.A., Keranen, K.M., Li, J., Delescluse, M., Mattei-Saliciup, G.A., 2015. Link between plate fabric, hydration and subduction zone seismicity in Alaska. *Nat. Geosci.* 8, 961–964.
- Sibson, R.H., Moore, J.M., Rankin, A.H., 1975. Seismic pumping – a hydrothermal fluid transport mechanism. *J. Geol. Soc. Lond.* 131, 653–659.
- Spiegelman, M., McKenzie, D., 1987. Simple 2-D models for melt extraction at mid-ocean ridges and island arcs. *Earth Planet. Sci. Lett.* 83, 137–152. melt1.
- Turcotte, D.L., Schubert, G., 1982. *Geodynamics: Applications of Continuum Physics to Geological Problems*. John Wiley, New York.
- Van Avendonk, H.J.A., Holbrook, W.S., Lizarralde, D., Denyer, P., 2011. Structure and serpentinization of the subducting Cocos plate offshore Nicaragua and Costa Rica. *Geochem. Geophys. Geosyst.* 12, Q06009. <http://dx.doi.org/10.1029/2011GC003592>.
- White, R.S., McKenzie, D., O’Nions, R.K., 1992. Oceanic crustal thickness from seismic measurements and rare earth element inversions. *J. Geophys. Res.* 97, 19683–19715.
- Wiens, D.A., Stein, S., 1983. Age dependence of oceanic intraplate seismicity and implications for lithospheric evolution. *J. Geophys. Res.* 88, 6455–6468.
- Wilkins, R.H., Fryer, G.J., Karsten, J., 1991. Evolution of porosity and seismic structure of upper oceanic crust: importance of aspect ratios. *J. Geophys. Res.* 96, 17981–17995.
- Yamasaki, T., Seno, T., 2003. Double seismic zone and dehydration embrittlement of the subducting slab. *J. Geophys. Res.* 108, 2212. <http://dx.doi.org/10.1029/2002JB001918>.